LUNAR COMPLEX CRATERS: REVISITING DEPTH-DIAMETER AND CENTRAL PEAK HEIGHT-DIAMETER RELATIONSHIPS. J. D. Kalynn[1], C. L. Johnson[1,2], O. S. Barnouin[3], G. R. Osinski[4], [1]Department of Earth, Ocean and Atmospheric Sciences, University of British Columbia, BC, V6T 1Z4, Canada, cjohnson@eos.ubc.ca. [2]Planetary Science Institute, Tucson, AZ 85719, USA, cjohnson@psi.edu. [3]The Johns Hopkins University Applied Physics Laboratory, Laurel, MD 20723, USA. [4] Departments of Earth Sciences and Physics and Astronomy, Centre for Planetary Science and Exploration, University of Western Ontario, ON, N6A 5B7, Canada.

Introduction: We use Lunar Orbiter Laser Altimeter (LOLA) topography data to revisit the depth (d)–diameter (D) and central peak height (h_{cp})–diameter relationships for fresh complex lunar craters [1]. Early studies of lunar crater morphometry investigated d versus D for simple and complex craters using shadow lengths from Earth-based telescope and Lunar Orbiter IV images, and stereophotogrammetry from Apollo metric images [2-6]. The d-D relationship was described by a power law, $d = AD^B$. Other studies investigated the morphology of the central peak, its height (h_{cp}), diameter, area and volume, and how these quantities scale with crater diameter [7-12].

With the exception of one earlier [13] and two recent [14-15] studies, previous analyses have been image-based due to the lack of absolute altimetric data of sufficient resolution to characterize crater topography. LOLA data allow investigations of the absolute topography of lunar complex craters, and in particular can resolve the topography of central peaks.

Dataset of Fresh Complex Craters: We used as our starting point a database of 8680 craters [16] and selected craters with reported ages that are Eratosthenian (3.2-1.1 Ga) or younger. We used a minimum crater diameter of 15 km: this excludes simple craters and includes some, but not all craters that have morphologies transitional between those of simple and complex craters.

We used Wide Angle Camera (WAC) monochromatic images from the Lunar Reconnaissance Orbiter Camera to check that our selected craters are "fresh". A crater was considered "fresh" if one or more of the following were observed: (1) impact melt on the crater floor and ejecta facies, (2) a well-defined crisp crater rim, (3) well-defined fault scarps on the crater walls, and/or (4) rays in the ejecta blanket. In addition, fresh craters needed to show no evidence for any of the following: (1) subsequent impacts in the interior or on the rim, (2) superposed ejecta from a nearby, younger crater, (3) an irregular shape, (4) post-impact volcanic fill, or (5) post-impact tectonic deformation.

The resulting 111 craters span the diameter range 15–167 km and are well-distributed geographically. We used the WAC images to classify each crater as complex or transitional. Both types exhibit terraced walls, but complex craters also exhibit clear central peaks protruding through the melt sheet. We identified the terrain impacted by each crater as mare, highland, mare-highland border, or South Pole Aitken Basin to allow investigations of variations in crater morphology with terrain type.

Topography Analyses: We characterized crater topography using the 512 ppd LOLA gridded dataset, and ensured that the 512 ppd (versus the 1024 ppd or the Reduced Data Records) grid has sufficient resolution for our analyses.

For each crater we estimated the rim and floor elevations, and their respective uncertainties. We first identified regions of impact melt in the WAC image, and used the topography of these regions to characterize the floor elevation. To characterize the rim elevation we used the GDR topography within an annulus bounded by 0.98D and 1.05D.

For the rim and floor regions we produced histograms of elevation, binned in 10 m intervals. We took the elevation characteristic of the floor (h_{floor}) to be the average of the modal (h_{mode}) and minimum (h_{min}) elevations and assigned an uncertainty of (h_{mode}-h_{min})/2. Similarly, we took the elevation characteristic of the rim (h_{rim}) to be the average of the modal (h_{mode}) and maximum (h_{max}) elevations and assigned an uncertainty of (h_{max}-h_{mode})/2. The crater depth, d, is the difference in floor and rim elevations, with an uncertainty equal to the square root of the sum of the squared uncertainties for the rim and the floor. The 10 m histogram bin width is greater than the vertical precision of the LOLA data, such that each bin contains many measurements, but is much smaller than the resulting uncertainty in the crater depth. We confirmed that our results are insensitive to the exact choice of bin width.

Of the 111 craters, 80 display central peaks characteristic of complex craters. The central peak height was calculated by taking the difference between the maximum elevation of the central peak and h_{floor}. Uncertainties in the central peak height were assigned as the uncertainty in h_{floor}; as these are much smaller than the variability in h_{cp} they were not used in our analyses.

Results: Our d-D results (Figure 1) show two trends consistent with earlier work. First, crater depth increases with increasing diameter. Second, complex craters on highland terrain are deeper than those on the mare terrain. Uncertainties in crater depths are dominated by variations in the crater rim height. The largest variations in rim height, and hence the largest uncertainties in our crater depths, are associated with craters that have impacted terrain with variations in pre-existing topography (e.g., highlands/mare bounda-

ries). These craters exhibit histograms of rim elevations that exhibit a broad spread of values, and this is captured in our estimate of crater rim uncertainty and hence depth uncertainty.

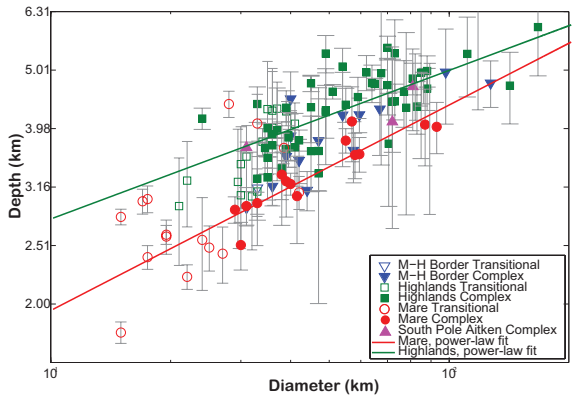

Figure 1. Log-log plot of depth (d) vs. diameter (D) for fresh young craters (symbols described in legend). Vertical gray bars denote depth uncertainties.

We performed a linear least squares regression in log-log space, to obtain power law relationships of the form $d = AD^B$ for complex craters on the mare and on the highlands. We determined the constants A and B, their 95% confidence intervals, and the root mean square misfit of each model to the corresponding data. Transitional craters were not included in the fits, so our models are strictly for young, fresh complex craters. Depth-diameter relationships for highland and mare complex craters are given by $d = 1.558D^{0.254}$ and $d = 0.870D^{0.352}$ respectively. The mare-highlands d-D difference is significant at the 95% confidence level. The South Pole Aitken population is consistent with the fits for the highlands craters. As expected mare-highland border complex craters have depths that range between those of mare and highland craters.

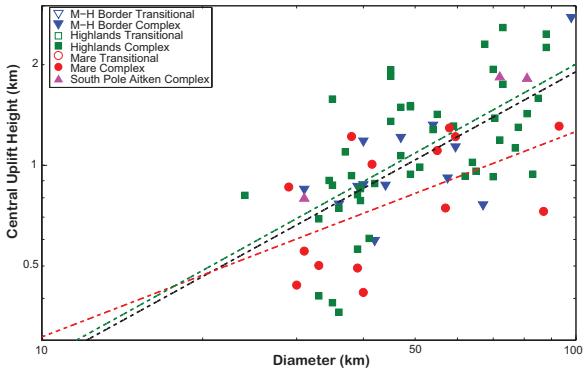

Figure 2. Log-log plot of central peak height vs. diameter for complex craters with D < 100 km (3 with D > 100 km not shown). Symbol color and type as in Figure 1. Dashed lines show best-fit power law relationships for highlands (green), mare (red) and all (black) young, fresh complex craters.

Central peak height also increases with increasing crater diameter (Figure 2). The central peak heights of mare craters are lower on average than those of highland craters over the same diameter range and this difference increases with increasing crater diameter. However, central peak heights show substantial variability at any given diameter, and this, combined with the small number of mare craters, means that a larger data set is needed to confirm terrain-type differences in the mean h_{cp}-D relationship.

Discussion and Summary: Complex craters on both the mare and the highlands are significantly deeper than previously reported for each terrain type [5], and the d-D power law exponent for highlands craters is also significantly less than previously published. We compared our data set with that of [5], and infer that the differences result from the inclusion of transitional and older and/or modified craters in previous work and/or limitations of the stereophotogrammetric and shadow-length data sets used in previous studies. In contrast, our depth estimate at Hausen crater is in excellent agreement with that in another recent study [13] and h_{cp} estimates in the two studies agree to within 1%, providing confidence in our results.

We suggest that the differences in mean d and h_{cp} as a function of crater diameter for highlands and mare craters result from differences in bulk physical properties of the terrain types. In particular, the more fragmented and porous megaregolith may allow the formation of deeper craters with larger central peaks in the highlands compared with those in the mare. Differences in layering in the target terrain may also contribute to differences in final crater morphology. We suggest that variations in d and h_{cp} at any given diameter for either mare or highlands terrain may reflect the effects of variations in impact parameters.

References: [1] Kalynn, J. et al. (2012) *GRL*, in press. [2] Baldwin, R. B. (1963), 488 pp., U. Chicago Press. [3] Baldwin, R. B. (1965), *Astronom. J.*, *70*, 545-547. [4] Pike, R.J. (1974), *GRL, 1*, 291–294. [5] Pike, R. J. (1980), *Proc. LPS 11th*, 2159–2189. [6] Pike, R.J. (1981), *LPS XII*, 845–847. [7] Wood, C. A. (1973), *Icarus*, *20*, 503-506. [8] Wood, C. A. and J. W. Head (1976), *Proc. LSC, 7*, 3629-3651. [9] Pike, R. J. (1977), *Impact and Explosive Cratering*, 489-509. [10] Wood, C. A., and L. Andersson (1978), *Proc. LPSC, 9*, 3669–3689. [11] Hale, W. S. and J. W. Head (1979), *Proc. LPSC 10th,* 2623–2633. [12] Hale, W. S., and R. A. F. Grieve (1982), *JGR, 87,* A65-A76. [13] Williams, K. K. and M. T. Zuber (1998), *Icarus*, *131*, 107–122. [14] Baker, D. M., et al. (2012), *JGR, 117*, doi:10.1029/2011JE004021. [15] Bray, V. J., et al. (2012), *GRL 39*, doi:10.1029/2012GL053693 [16] Losiak, A. et al. (2009), *LPS*, *XXXX*, #1532